



Photochemical reactivity of two gold(I) dinuclear complexes, *cis/trans*-(Au^pNBT)₂dppee: Isomerization for the *cis*-(Au^pNBT)₂dppee isomer, radical substitution for *trans*-(Au^pNBT)₂dppee

Janet B. Foley^{a,*}, Angela Herring^a, Bo Li^b, Evgeny V. Dikarev^{b,1}

^a Bennington College, Bennington, VT 05201, USA

^b University at Albany, SUNY, Albany, NY 12222, USA

ARTICLE INFO

Article history:

Received 24 January 2012

Received in revised form 10 March 2012

Accepted 14 March 2012

Available online 27 March 2012

Keywords:

Gold
X-ray crystal structure
Photochemistry
Gold–gold bonding
Luminescence

ABSTRACT

Two complexes, *cis* (**1**) and *trans* (**2**) (Au^pNBT)₂dppee (pNBT = *p*-nitrobenzenethiol; dppee = bis(diphenylphosphino)ethylene) have been synthesized and characterized. X-ray diffraction studies reveal that *cis*-(Au^pNBT)₂dppee has an intramolecular gold–gold distance of 3.0036(3) Å while the *trans*-(Au^pNBT)₂dppee crystal is a dimer with an intermolecular gold–gold distance of 3.1201(4) Å. We have used UV–Vis spectroscopy, ¹H NMR, and ³¹P {¹H} NMR to investigate the photochemical reactivity of both complexes. In a range of organic solvents with $\lambda > 230$ nm *cis*-(Au^pNBT)₂dppee readily isomerizes to the *trans* isomer. Under these same conditions, the *trans* isomer does not isomerize to *cis*-(Au^pNBT)₂dppee, but undergoes a photochemical substitution reaction. In chlorinated solvents (CH₂Cl₂, CH₂Cl) *trans*-(Au^pNBT)₂dppee reacts to form *trans*-(AuCl)₂dppee (**3**) which crystallizes into an extended chain of molecules linked via intermolecular gold–gold distances of 3.0203(2) Å. TDDFT calculations support the observed experimental results. We propose that at high energies the reaction is initiated by chlorine radicals from direct photolysis of the solvent. At longer wavelengths the excited state of the metal complex is the photoactive species, abstracting a chlorine radical from the solvent.

© 2012 Elsevier B.V. All rights reserved.

1. Introduction

Gold(I) compounds have been used to treat rheumatoid arthritis [1] for over 50 years and, more recently, some of the same compounds have shown potential as anticancer drugs [2]. Some studies propose that these gold complexes inhibit selenoenzymes and that thiol ligand exchange on the gold plays a crucial role [3]. Some gold thiol rheumatoid arthritis drugs have shown sensitivity to light [4] and although these drugs are not widely used now, the nature of that photochemical instability has implications for other phosphine–gold–thiol drugs. The current interest in gold complexes extends beyond their medicinal applications. The binding of gold to sulfur is the basis of self assembled monolayers applications [5], biosensor devices [6], and attachments to gold nanoparticles [7]. Gold(I) complexes have shown promise as catalysts for water soluble addition reactions, rearrangements, and many other reaction

Abbreviations: pNBT, *para*-nitrobenzenethiol; dppee, bis(diphenylphosphino)ethylene; *p*-ClBT, *para*-chlorobenzenethiol; *p*-NH₂BT, *para*-aminobenzenethiol; pTC, *para*-thiocresol; hfac, 111555hexafluoro-2*4-pentanedionato; TG, tetraglyme 2581114-pentaoxapentadecane.

* Corresponding author. Tel.: +1 802 440 4463.

E-mail addresses: jfoley@bennington.edu (J.B. Foley), dikarev@albany.edu (E.V. Dikarev).

¹ Tel.: +1 518 442 4401.

types [8]. Gold–gold interactions, the attraction between gold atoms in solid state structures or in solution, can provide scaffolding for supramolecular constructions [9] as well as affect the luminescent properties of gold molecules [10]. The ligand replacement characteristics, the stability of gold–sulfur bonds, and the photochemical properties of gold(I) complexes are basic concepts that directly relate to advancement in these areas of research.

Previous work showed that *cis*-(AuX)₂dppee complexes (X = Cl, Br, I), that have short intramolecular gold–gold distances, isomerize to the *trans* isomer when exposed to light, both UV and $\lambda > 320$ nm [11]. Quantum yields, measured at 334 nm for the halides were found to be $\Phi = 0.204 \pm 0.062$ (Cl), 0.269 ± 0.092 (Br), 0.363 ± 0.055 (I) [12]. *Ab initio* calculations [13] attribute the isomerization to a π^* excited state accessible to the *cis* isomer because of the intramolecular gold–gold interaction. Because gold–gold bonding is crucial for the isomerization in the halide series and these weak interactions are predicted to be enhanced by “soft” ligands [14], the photochemical properties of a thiol analog of *cis/trans*-(AuX)₂dppee presented a natural extension of our previous study.

Most of the photochemistry of Au(I) has been redox, resulting in disproportionation to Au(0) and Au(III). A few extensive reviews have outlined these photochemical studies [15]. Gold complexes can also form three coordinate structures by oxidative addition of halides or alkylhalides to form gold(II) complexes. This

mechanism is most commonly seen for dinuclear substrates with bridging ligands [16], dithiocarbamates [17], and phosphine annular ions [18]. Radical initiated oxidative addition has also been reported in both gold complexes and with other metals [19]. Many metals (Pt [20], Ru [21], Fe [22], Au [15]) have been shown to undergo photochemical reactions in chlorinated solvents. These reactions can be initiated by homolytic cleavage of the solvent, by excitation of the metal complex, or by CTTS (charge transfer to solvent) transitions. There can also be solvent initiated and metal centered reactions happening in the same system. The reactivity depends on the solvent C–Cl bond energy, which decreases along the series $\text{CH}_2\text{Cl}_2 > \text{CHCl}_3 > \text{CCl}_4$.² An experiment by Hoggard and co-workers [23] reevaluates some previous examples of iron dithiocarbamate photochemistry, proposing that at high energies in chlorinated solvents, a solvent-initiated process predominates and at lower energies a metal-initiated process generates the radicals, both resulting in the same product. Photosubstitution without change in metal oxidation state is not common but Hoggard and co-worker [24] suggest a direct solvent bond homolysis for the photosubstitution of $[\text{Ru}(\text{bpy})_2(\text{N}_3)_2]$ to $[\text{Ru}(\text{bpy})_2(\text{Cl})_2]$ with no participation of the metal complex because the reaction does not happen at longer wavelengths where the complex absorbs.

Au(I) is a formally closed shell metal ion which eliminates the option of d–d transitions that might happen at low energies but ligands, particularly reducing thiols, can push the lowest energy absorption into the visible, making it likely that the lowest energy transition is an LMCT (ligand to metal charge transfer) [25]. Relativistic effects [26] cause the 6s and 6p orbitals on the gold to be close in energy to the formally filled 5d and make metal orbitals potentially available to the excited state. Many gold(I) complexes luminesce under mild conditions. This property has been the basis of systems that detect ions in solution [27], the presence of organic solvents [6b], and many other applications. The possibility of low energy transitions, the electronic effects of gold–gold interactions, and the heavy atom properties of gold combine to make these complexes ideal substrates for probing the basic chemistry of this unique metal.

Our present study describes (1) the synthesis and characterization of the *cis* and *trans*-(AupNBT)₂dppee complexes, (2) the photochemical isomerization of *cis*-(AupNBT)₂dppee, (3) the photochemical ligand substitution of *trans*-(AupNBT)₂dppee, and (4) DFT and TDDFT calculations performed to explain the experimental results.

2. Experimental

2.1. General methods

$\text{HAuCl}_4 \cdot 3\text{H}_2\text{O}$, *p*-nitrobenzenethiol and other reagents were purchased from Alfa Aesar or Aldrich and used as is. Syntheses were carried out under nitrogen using standard Schlenk line techniques and adapted from previously reported procedures [11]. ¹H NMR and ³¹P {¹H} NMR spectra were recorded on a Varian 200 MHz or a Varian 300 MHz instrument in CDCl_3 or CD_2Cl_2 . Chemical shifts are quoted relative to TMS for the ¹H NMR or 85% H_3PO_4 for ³¹P {¹H} NMR. C, H, N, Cl analyses were conducted by Desert Analytics, part of Columbia Analytical Services, Tucson, Arizona. Crystals for X-ray analysis were grown by slow diffusion of ethyl ether into a methylene chloride solution of the gold complex. Absorption spectra were recorded on an Ocean Optics 2000 spectrometer. Emission and excitation spectra were measured on a Jobin Hovan fluorimeter in solution (CH_2Cl_2) or in the solid state as KBr mixtures at room temperature.

² In addition to the C, H, Cl analysis, there was a small percentage of sulfur (0.11%) which might indicate some residual starting material or disulfide in the product that was not evident in the ³¹P {¹H} NMR or the ¹H NMR.

2.2. Photolysis reactions

All reactions were subjected to a 100 W Oriel photolysis lamp and monitored by UV–Vis or NMR spectroscopy. Samples were photolyzed in quartz cuvettes allowing wavelengths of the Hg Arc lamp greater than 230 nm to illuminate the samples. A 420 nm Oriel cutoff filter: (transmittance 440–2500 nm; 75% transmittance at 440 nm) was used for the low energy excitations. Reactions were carried out in air except when nitrogen is specified. In some cases the photolysis in quartz used a 14×2 mm mask on the cuvette sample holder to limit photon flux to slow the reaction enough to observe more detail.

2.3. Synthesis of *cis*-(AupNBT)₂dppee (1)

Cis-(AuCl)₂dppee was synthesized by literature methods [28]. The white solid (0.255 g, 0.29 mmol) was degassed and dissolved in degassed methylene chloride. In a separate flask 2.5 equivalents (0.1147 g, 0.73 mmol) of *p*-nitrobenzenethiol were dissolved in ethanol and put under a nitrogen atmosphere. Ethanolamine (0.0445 ml, 0.73 mmol) was added to deprotonate the ligand. The solution turned bright red–orange and was added via cannula to the solution of the gold complex. After stirring for 1 h in ice, the solvent was evaporated under vacuum and an orange solid was recovered. The product was recrystallized from methylene chloride/hexanes. Average yield = 78%. Elemental Anal. Calc. for $\text{C}_{38}\text{H}_{30}\text{Au}_2\text{N}_2\text{O}_4\text{P}_2\text{S}_2$: C, 41.53; H, 2.73; N, 2.55. Exp.: C, 41.57; H, 2.68; N, 2.5%. ¹H NMR (CD_2Cl_2 , 300 MHz) $\delta = 7.3$ – 7.65 (m), $\delta = 7.74$ (d) { $J = 9$ Hz}. ³¹P {¹H} NMR $\delta = 19.5$ ppm (s); 85% $\text{H}_3\text{PO}_4 = 0$ as reference.

2.4. Synthesis of *trans*-(AupNBT)₂dppee (2)

Trans-(AuCl)₂dppee was synthesized according to literature methods [29]. 0.255 g, (0.29 mmol) of the relatively insoluble white compound was degassed, put under nitrogen and dissolved in degassed methylene chloride to form a white slurry. In a separate flask 2.5 equivalents (0.1147 g, 0.73 mmol) of *p*-nitrobenzenethiol were dissolved in ethanol and put under a nitrogen atmosphere. Ethanolamine (0.0445 ml, 0.73 mmol) was added to deprotonate the ligand. The solution turned bright red–orange and was added via cannula to the solution of the gold complex which turned transparent yellow. After stirring for one hour in ice, the solvent was evaporated under vacuum and a yellow, air stable solid was recovered. Product was recrystallized in methylene chloride/hexane to give an average of 67% yield. Elemental Anal. Calc. $\text{C}_{38}\text{H}_{30}\text{Au}_2\text{N}_2\text{O}_4\text{P}_2\text{S}_2$: C, 41.53; H, 2.73; N, 2.55. Exp.: C, 41.31; H, 3.09; N, 2.99%. ¹H NMR: (CD_2Cl_2 , 300 MHz) $\delta = 7.545$ – 7.795 (m), $\delta = 7.86$ (d) ($J = 9$ Hz); ³¹P {¹H} NMR $\delta = 35.6$ ppm (s); 85% $\text{H}_3\text{PO}_4 = 0$ as reference.

2.5. Characterization of the product, *trans*-(AuCl)₂dppee (3) from photolysis of *trans*-(AupNBT)₂dppee

Crystals for the X-ray analysis were collected from the slow diffusion recrystallization (methylene chloride/ethyl ether) of the product, identified as *trans*-(AuCl)₂dppee, of the photolysis in quartz of *trans*-(AupNBT)₂dppee in methylene chloride. Elemental Anal. Calc. for $\text{C}_{26}\text{H}_{22}\text{Au}_2\text{Cl}_2\text{P}_2$: Calc: C, 36.20; H, 2.56; Cl, 8.25. Exp.: C, 36.37; H, 2.97; Cl, 8.40%.³ ¹H NMR: (CD_2Cl_2 , 300 MHz) $\delta = 7.66$ – 7.53 (m), $\delta = 7.114$ (t) ($J = 20$ Hz), ³¹P {¹H} NMR (CD_2Cl_2): $\delta = 29.6$ ppm(s); 85% $\text{H}_3\text{PO}_4 = 0$ as reference.

³ C–Cl bond dissociation energy (kJ mol^{-1}) from NIST: $\text{CH}_2\text{Cl}_2 = 307.8$, $\text{CHCl}_3 = 299.15$, $\text{CCl}_4 = 284.1$.

2.6. *Ab initio* computations

Ground state electronic structures were calculated using the density functional (DFT) application in the GAUSSIAN 09 program [30] on model compounds that substituted hydrogens for the phenyl rings in the phosphine. Singlet and triplet excited states were calculated using the TDDFT application in the same program. The B3LYP exchange–correlation function was used with the LANL2DZ basis set for gold with an additional f function ($\alpha_f = 0.2$) in the valence shell of the gold. A 6-311G(d,p) basis set was used for the non-metal atoms. Full geometry optimizations were performed for all molecules in the ground state and single point calculations were used to examine the excited states. The Polarized Continuum Model using the integral equation formula (IEF-PCM) was used to simulate the solvent, methylene chloride, for the *trans*-(AupNBT)₂dppee calculation because the nature of the reaction suggested more reliance on the nature of the solvent and it gave better agreement with the experimental results. Solvent parameters were not used in the *cis*-(AupNBT)₂dppee calculation. No symmetry constraints were imposed. GAUSSVIEW 05 was used for visualization.

2.7. X-ray crystallographic procedures

Selected single crystals suitable for X-ray crystallographic analysis were used for structural determination. The X-ray intensity data were measured at 173(2) K (Bruker KRYOFLEX) on a Bruker SMART APEX CCD-based X-ray diffractometer system equipped with a Mo-target X-ray tube ($\lambda = 0.71073$ Å) operated at 1800 W power. The crystals were mounted on a goniometer head with silicone grease. The detector was placed at a distance of 6.14 cm from the crystal. For each experiment a total of 1850 frames were collected with a scan width of 0.3° in ω and an exposure time of 20 s/frame. The frames were integrated with the Bruker SAINT Software package using a narrow-frame integration algorithm to a maximum 2θ angle of 56.54° (0.75 Å resolution). The final cell constants are based upon the refinement of the XYZ-centroids of several thousand reflections above $20 \sigma(I)$. Analysis of the data showed negligible decay during data collection. Data were corrected for absorption effects using the empirical method (SADABS). The structures were solved and refined by full-matrix least-squares procedures on $|F^2|$ using the Bruker SHELXTL (version 6.12) software package. The coordinates of metal atoms for the structures were found in direct method E maps. The remaining atoms were located after an alternative series of least squares cycles and difference Fourier maps. For alkenes in **1**, **2** and **3**, hydrogen atoms were located and refined independently while the remaining hydrogen atoms were included in idealized positions for structure factor calculations. Anisotropic displacement parameters were assigned to all non-hydrogen atoms, except solvent molecules in *trans*-(AuCl)₂dppee. Relevant crystallographic data are summarized in Table 1.

3. Results and discussion

3.1. Synthesis, crystal structure and absorption spectrum of *cis*-(AupNBT)₂dppee (**1**)

Synthesis was by chloride substitution of *cis*-(AuCl)₂dppee with deprotonated *p*-nitrobenzenethiol in methylene chloride to form the dinuclear *cis*-(AupNBT)₂dppee, an orange, air stable solid that luminesced red–orange under UV light and was soluble in most organic solvents. The product was characterized by elemental analysis, X-ray crystal analysis, UV–Vis, ¹H NMR, and ³¹P {¹H} NMR spectroscopy. The synthesis highlights the unique nature of the *p*-nitrobenzenethiol because attempts to synthesize similar *cis* complexes in our lab using other benzenethiol ligands, *p*-thiocresol,

p-aminobenzenethiol, and *p*-chlorobenzenethiol, were unsuccessful, although the *trans* counterparts were made in good yields. The UV–Vis spectrum shows a high energy absorbance with a maximum at 236 nm ($\epsilon = 4.37 \times 10^4 \text{ M}^{-1} \text{ cm}^{-1}$) that has been assigned to phenyl transitions in the phosphine based on comparison to similar compounds [31]. There is also a broad low energy peak with a maximum at 400 nm ($\epsilon = 3.25 \times 10^4 \text{ M}^{-1} \text{ cm}^{-1}$), assigned to the *p*-nitrobenzenethiol ligand, based on comparison to spectra of other molecules in this series [11] as well as other experiments with this ligand [32]. The extended conjugation of the nitrobenzenethiol ligand is likely responsible for this low energy absorbance compared to other benzene thiol ligands. *Ab initio* calculations indicate that the percentage of sulfur in the HOMO of this ligand is greater than for any other of the common aromatic substituents (48.1%) [33] and the extreme electron withdrawing nature of the nitro substituent stabilizes the HOMO of this ligand compared to other benzenethiols. The stability of the HOMO appears to allow for productive overlap of the sulfur orbitals with the gold while other ligands (*p*-ClBT, *p*-NH₂-BT, *p*TC) do not.

The primary feature of the crystal structure is the 3.0037(3) Å gold–gold distance, Fig. 1 implying that there are significant intramolecular gold–gold interactions [34]. The linear geometry of the P–Au–S axis is slightly distorted to $174.10(3)^\circ$ in order to maximize the gold–gold attraction. There are no close intermolecular gold–gold interactions in the unit cell. The “arms” of the molecule are not parallel, but are offset by 74.4° , minimizing the repulsions that might occur between the *p*-nitrobenzenethiol ligands. Table 2 compares specific details with other similar crystal structures.

3.2. Photochemistry of *cis*-(AupNBT)₂dppee (**1**)

When a methylene chloride solution of *cis*-(AupNBT)₂dppee (**1**) was exposed to light, in air or under nitrogen, it isomerized to the *trans* isomer. The isomerization occurred at wavelengths greater than 230 nm and when a 420 nm cutoff filter was used. The reaction was followed by ¹H NMR, ³¹P {¹H} NMR, and UV–Visible spectroscopy. The UV–Visible spectrum in methylene chloride, Fig. 2, shows the isomerization process as the *cis* isomer ($c = 4.27 \times 10^{-5} \text{ M}$), with $\lambda_{\text{max}} = 400 \text{ nm}$ ($\epsilon = 3.25 \times 10^4 \text{ M}^{-1} \text{ cm}^{-1}$) isomerized to the *trans* ($\lambda_{\text{max}} = 385 \text{ nm}$; $\epsilon = 3.3 \times 10^4 \text{ M}^{-1} \text{ cm}^{-1}$) in a quartz cuvette. Although the absorptivity of the *cis* and *trans* isomers is about the same, the peak decreases quickly even as the isomerization proceeds because the *trans*-(AupNBT)₂dppee undergoes a further photoreaction (vide infra). Based on a weighted average calculation, at 40 s there is 28% of the *cis*-(AupNBT)₂dppee remaining while 72% of the initial $4.27 \times 10^{-5} \text{ M}$ solution isomerized to the *trans* isomer. However, at 40 s, some of the *trans* compound has reacted further, evidenced by the decrease in the absorbance at 385 nm. The isomerization suggests that the excited state has π^* character, similar to the other *cis* complexes in this series, [X = Cl, Br, I] [11]. In the ³¹P {¹H} NMR spectrum the initial peak at 19.5 ppm diminishes as a broad peak around 35.0 ppm grows in, indicating formation of *trans*-(AupNBT)₂dppee. As the reaction proceeds several intermediate peaks are observed at 33, 32, and 31 ppm perhaps representing intermediates or mixtures generated in the photochemical reaction of *trans*-(AupNBT)₂dppee. This supports our observation from the UV–Vis experiment that the *trans*-(AupNBT)₂dppee reacts as soon as it is produced from the isomerization.

3.3. Synthesis, crystal structure and absorbance spectrum of *trans*-(AupNBT)₂dppee (**2**)

The *trans*-(AupNBT)₂dppee complex was synthesized by ligand substitution of the deprotonated *p*-nitrobenzenethiol ligand with *trans*-(AuCl)₂dppee in methylene chloride. The product was a yellow air-stable solid that luminesced bright orange under UV light.

Table 1Crystallographic data and structure refinement parameters for *cis*-(AupNBT)₂dppee·2CH₂Cl₂ (**1**·2CH₂Cl₂), *trans*-(AupNBT)₂dppee·CH₂Cl₂ (**2**·CH₂Cl₂), and *trans*-(AuCl)₂dppee (**3**).

| | 1 ·2CH ₂ Cl ₂ | 2 ·CH ₂ Cl ₂ | 3 |
|---|---|---|--|
| Formula | C ₄₀ H ₃₄ Au ₂ Cl ₄ N ₂ O ₄ P ₂ S ₂ | C ₃₉ H ₃₂ Au ₂ Cl ₂ N ₂ O ₄ P ₂ S ₂ | C ₂₆ H ₂₂ Au ₂ Cl ₂ P ₂ |
| Formula weight | 1268.48 | 1183.56 | 861.21 |
| Crystal system | monoclinic | triclinic | monoclinic |
| Space group | C 2/c | Pī | C 2/c |
| <i>Unit cell dimensions</i> | | | |
| <i>a</i> (Å) | 18.3627(10) | 12.3682(10) | 16.5106(6) |
| <i>b</i> (Å) | 14.1750(8) | 13.1123(10) | 15.0625(5) |
| <i>c</i> (Å) | 16.5005(9) | 14.6372(12) | 11.3460(4) |
| α (°) | 90.00 | 66.7240(10) | 90.00 |
| β (°) | 102.5050(10) | 68.7770(10) | 117.0630(10) |
| γ (°) | 90.00 | 80.1530(10) | 90.00 |
| <i>V</i> (Å ³) | 4193.0(4) | 2031.6(3) | 2512.69(15) |
| <i>Z</i> | 4 | 2 | 4 |
| ρ (g cm ⁻³) | 2.009 | 1.935 | 2.277 |
| μ (mm ⁻¹) | 7.464 | 7.568 | 12.017 |
| λ (Å) | Mo K α (0.71073) | Mo K α (0.71073) | MoK α (0.71073) |
| Transmission factors | 0.4006–0.5866 | 0.2994–0.7517 | 0.0622–0.4465 |
| <i>T</i> (K) | 173(2) | 173(2) | 173(2) |
| Data/restraints/parameter | 4556/0/251 | 8674/0/455 | 2749/11/178 |
| <i>R</i> ₁ ^a , <i>wR</i> ₂ ^b <i>I</i> > 2 σ (<i>I</i>) | 0.0220, 0.0565 | 0.0420, 0.1091 | 0.0168, 0.0439 |
| All data | 0.0250, 0.0578 | 0.0523, 0.1155 | 0.0174, 0.0443 |
| Quality-of-fit ^c | 1.054 | 1.059 | 1.065 |

^a $R_1 = \sum |F_o| - |F_c| / \sum F_o$.^b $wR_2 = [\sum [w(F_o^2 - F_c^2)^2] / \sum [w(F_o^2)^2]]^{1/2}$.^c Quality-of-fit = $[\sum [w(F_o^2 - F_c^2)^2] / (N_{obs} - N_{params})]^{1/2}$, based on all data.**Table 2**Selected bond lengths and bond angles for (**1**)*cis* and (**2**)*trans* and (**3**)*trans*-(AuCl)₂dppee compared to other gold(I) phosphine complexes.

| Complex | Au–Au (Å) | P–Au (Å) | X–Au (Å) | P–Au–X (°) | Au2–Au1–P1 (°) | Ref. |
|--|---------------------------------------|----------------|-----------|------------|----------------|-----------|
| <i>cis</i> -(AupNBT) ₂ dppee (1) | 3.0036(3) | 2.2717(8) | 2.3120(8) | 174.10(3) | 82.10(2) | This work |
| <i>trans</i> -(AupNBT) ₂ dppee (2) | 3.1201(4) | 2.2665(18) | 2.308(2) | 171.25(7) | 98.12(5) | This work |
| | intermolecular | 2.2597(17) | X = S | 171.41(7) | 94.92(5) | |
| <i>trans</i> -(AuSPh) ₂ dppee | 3.023(2) | 2.274(9) | 2.30(1) | 174.3(3) | | a |
| | intermolecular | 2.24(1) | X = S | | | |
| (AuCl) ₂ dppee | 3.189(1) | 2.242(6) | 2.314(5) | 175.4(2) | 108.0(2) | b |
| | dppee = bis(diphenyl)phosphino ethane | intermolecular | X = Cl | | | |
| <i>cis</i> -(AuCl) ₂ dppee | 3.05(1) | 2.238(5) | 2.288(7) | 175.4(2) | | c |
| | | | X = Cl | | | |
| <i>trans</i> -(AuCl) ₂ dppee | 3.043(1) | 2.235(2) | 2.291(2) | 173.5(1) | | d |
| | intermolecular | | X = Cl | | | |
| <i>cis</i> -(AuI) ₂ dppee | 2.9526(5) | 2.253(2) | 2.5629(9) | 170.36(6) | 94.21(6) | e |
| | | | X = I | | | |
| <i>trans</i> -(AuI) ₂ dppee | 3.2292(7) | 2.250(2) | 2.5435(8) | 174.81(6) | 101.42(6) | e |
| | intermolecular | | X = I | | | |
| <i>trans</i> -(AuCl) ₂ dppee (3) | 3.0203(2) | 2.2412(7) | 2.2928(7) | 173.92(3) | 101.823(18) | This work |
| | Photoproduct | intermolecular | X = Cl | | | |

a Onaka et al. [35].

b Bates and Waters [45].

c Jones [28].

d Eggleston et al. [29].

e Foley et al. [12].

The product was verified by elemental analysis, X-ray crystallography, ³¹P {¹H} NMR and ¹H NMR and UV–Vis spectroscopy. The main feature of the crystal structure is the dimer unit with a short (3.1201 Å) intermolecular gold–gold distance and some π – π stabilization from the interaction of two phenyl rings from the diphenylphosphine backbone (Fig. 3). There are no other close gold–gold contacts in the unit cell which includes a methylene chloride molecule. The *p*-nitrobenzenethiol ligands are nearly perpendicular to each other in the dimer. The P(1)–Au(1)–S(2) and the P(2)–Au(2)–S(1) bond angles (171.27(6) and 171.42(6), respectively) are distorted from linear, presumably to enhance the gold–gold interaction. Dimer structures in other *trans* complexes with the dppee backbone are not unusual. Eggleston et al. [29] report an intermolecular gold–gold distance of 3.043 Å

between two molecules of *trans*-(AuCl)₂dppee in the crystal. In the unit cell of *trans*-(AuI)₂dppee [12] there are two dimers, each with an intermolecular gold–gold distance of 3.2292 Å. A crystal structure of an analogous thiophenol, *trans*-(AuSPh)₂dppee [35], shows an infinite chain forming a two-dimensional network held together by intermolecular gold–gold interactions and π – π interactions of the SPh ligands. As in our experience, Onaka et al. [36] could not synthesize the *cis*-(AuSPh)₂dppee by ligand substitution.

The absorption spectrum is dominated by a broad low energy peak with a maximum wavelength at 385 nm ($\epsilon = 3.3 \times 10^4$ M⁻¹ cm⁻¹). As in the *cis* isomer, the *trans*-(AupNBT)₂dppee has a high energy absorbance at 236 nm ($\epsilon = 5.1 \times 10^4$ M⁻¹ cm⁻¹) that is common for complexes with phenylphosphine ligands.

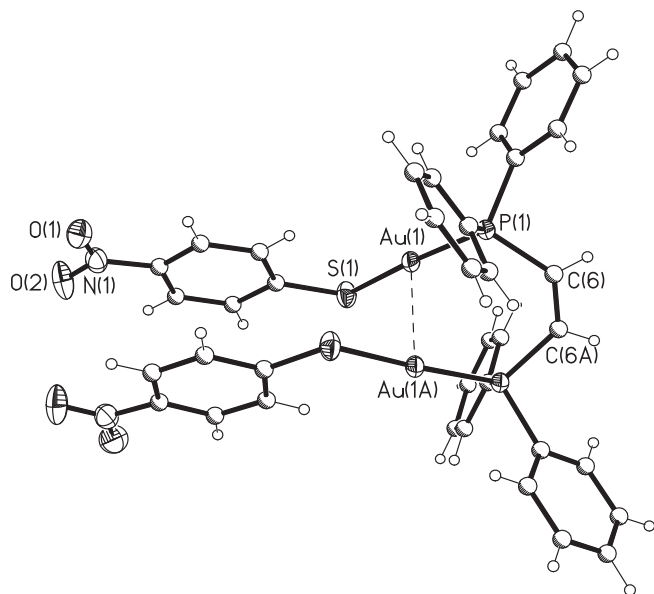


Fig. 1. Molecular structure of *cis*-(AupNBT)₂dppee (**1**). Atoms are represented by thermal ellipsoids at the 40% probability level. See Table 2 for selected distances (Å) and angles (°).

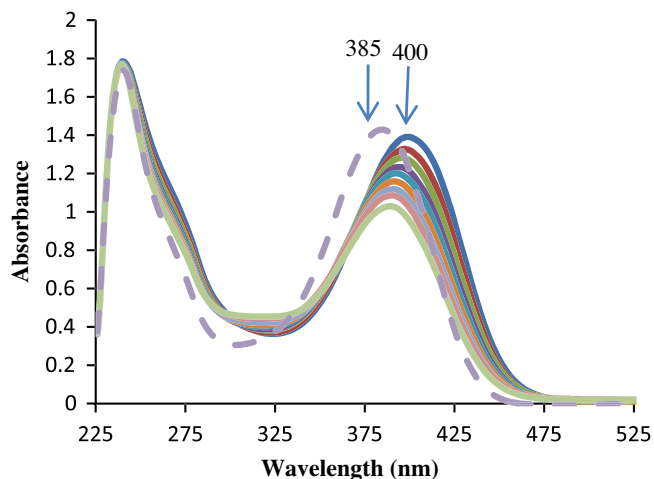
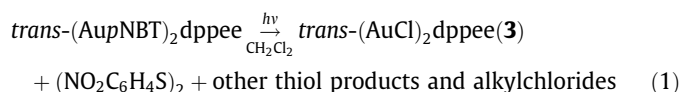


Fig. 2. Photolysis of *cis*-(AupNBT)₂dppee (**1**) in CH₂Cl₂: *t* = 0–40 s; $\lambda > 230$ nm; λ_{\max} *cis*-(AupNBT)₂dppee = 400 nm; λ_{\max} *trans*-(AupNBT)₂dppee = 385 nm. Light intensity was reduced by using a mask on the sample holder to slow the reaction and allow more detail to be observed. *Trans*-(AupNBT)₂dppee (Dashed line) overlay for comparison only.

3.4. Photochemistry of *trans*-(AupNBT)₂dppee (**2**)

While investigating the photochemical reaction of *cis*-(AupNBT)₂dppee, we noted that the very rapid isomerization reaction was followed by a photoreaction of *trans*-(AupNBT)₂dppee. Other *trans* complexes in this series, *trans*-(AuX)₂dppee [X = Cl, Br, I, *p*-thiocresol, SCN]⁴ did not exhibit further photochemical reaction in the time frame of the isomerization experiments (several minutes). However, after prolonged photolysis (18 min in a quartz cuvette) we did observe evidence (reduced gold) that the *trans*-(AuCl)₂dppee may have disproportionated.

When *trans*-(AupNBT)₂dppee was photolyzed in a variety of organic solvents (ACN, DMF, acetone, THF) a photochemical reaction occurred evidenced by the decrease in the low energy absorbance ($\lambda_{\max} \approx 385$ nm) in the UV–Vis spectrum. The peak maximum red shifted slightly with more polar solvents, a phenomenon also observed by others for gold complexes with the *p*NBT ligand [32a]. Only when *trans*-(AupNBT)₂dppee was photolyzed in a chlorinated solvent (CH₂Cl₂ or CHCl₃) were we able to separate and identify some of the products. We used CH₂Cl₂ for better solubility of the complex and easier analysis in the ¹H NMR. Based on UV–Vis data, ¹H NMR, and ³¹P {¹H} NMR, and X-ray analysis, the products of the photolysis of *trans*-(AupNBT)₂dppee were identified as *trans*-(AuCl)₂dppee and various radical thiol products including the 4,4'-dinitrophenyldisulfide. Eq. (1) summarizes these results.



Photolysis of *trans*-(AupNBT)₂dppee was carried out using two wavelength ranges, (a) in quartz ($\lambda > 230$ nm), and (b) the 420 nm filter, in order to define conditions necessary for the formation of the *trans*-(AuCl)₂dppee product. Fig. 4 illustrates two typical experiments: the 385 nm peak of the original *trans*-(AupNBT)₂dppee complex decreases as a peak at 320 nm grows in, with an isosbestic point at 335 nm.

3.5. Characterization of the products of the photolysis of *trans*-(AupNBT)₂dppee

The product of the photolysis of *trans*-(AupNBT)₂dppee was collected, recrystallized and separated into a crystal fraction and a solvent fraction. The ¹H NMR of the crystal fraction, (see Supplementary data, Fig. S-1a) identified as *trans*-(AuCl)₂dppee (**3**), clearly shows peaks for the dppee phenyl hydrogens and a distinct triplet ((CD₂Cl₂, 300 MHz) 7.112 ppm; *J* = 20.0 Hz) related to the hydrogens on the ethylene backbone that is typical for these *trans* complexes [11]. The ³¹P{¹H}NMR peak is at 29.6 ppm. Both spectra are identical to an independently synthesized sample of *trans*-(AuCl)₂dppee and the elemental analysis was consistent with the formation of *trans*-(AuCl)₂dppee. However, it is interesting to note that the crystals we obtained appeared as light-yellow rectangles while the original crystals of *trans*-(AuCl)₂dppee [29] were reported as white needles representing a dimer with intermolecular gold–gold distances of 3.043 Å. The crystal structure of our *trans*-(AuCl)₂dppee photoproduct (**3**) (Fig. 5) sheds some light on this discrepancy by revealing an infinite chain of *trans*-(AuCl)₂dppee molecules with gold–gold distances of 3.0203 Å. It is not unusual for gold complexes to form polymorphs when crystallizing [37] and the extended chain of gold–gold interactions could result in a red shift in absorbance causing a slight change in color. In solution the sample's ¹H NMR spectrum was identical to an authentic sample of *trans*-(AuCl)₂dppee. The yield of recrystallized *trans*-(AuCl)₂dppee photoproduct varied from 40% to 60%. There was some evidence of unidentified insoluble bits in the product. The crystal structure is similar to that of Eggleston et al. with comparative Au–Cl bond lengths and P–Au–Cl bond angles. There are slightly different Au–P bond lengths: 2.2413(7) Å for our photoproduct compared to 2.235(2) Å for Eggleston's crystal structure.

The recrystallized thiol fraction was examined by ¹H NMR but the interpretation is less definitive than the *trans*-(AuCl)₂dppee samples (See Supplementary data, Fig. S-1b). There are a series of doublets, two of which can be identified as the 4,4'-dinitrophenyldisulfide, one at 8.187 ppm (*J* = 9.0 Hz) and the other at 7.655 ppm (*J* = 9.0 Hz), identical to an authentic sample of the disulfide. There are other doublets, one at 8.265 (*J* = 9.0 Hz),

⁴ See Ref. [11]; *trans*-(Auptc)₂dppee and *trans*-(AuSCN)₂dppee photolysis are from unpublished results in our lab.

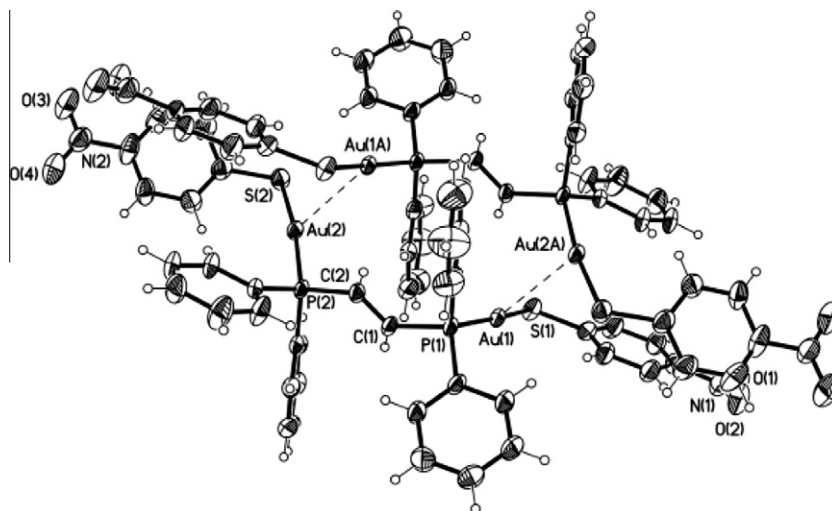


Fig. 3. Molecular structure of *trans*-(AupNBT)₂dppee (**2**). Atoms are represented by thermal ellipsoids at the 40% probability level. See Table 2 for selected distances (Å) and angles (°).

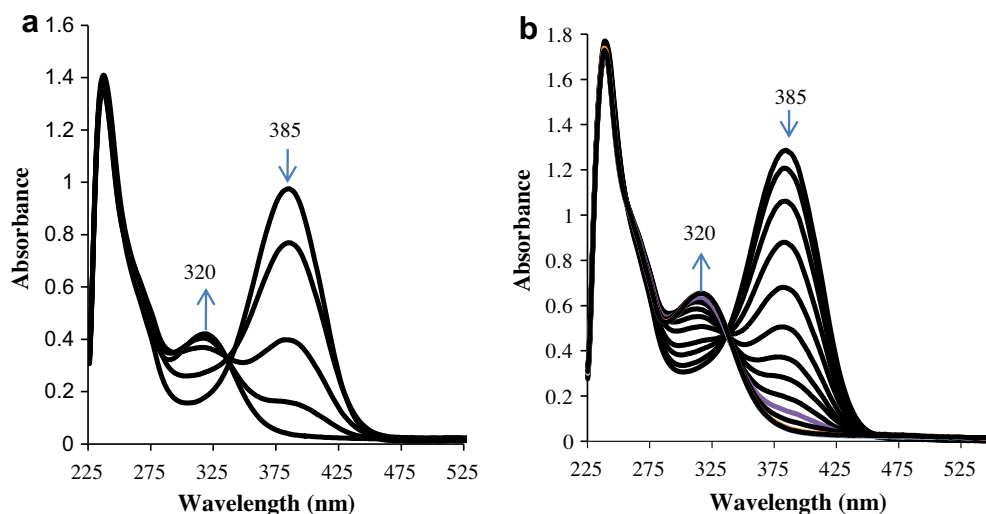


Fig. 4. (a) Photolysis of *trans*-(AupNBT)₂dppee (**2**) in CH₂Cl₂: *t* = 0–20 s; $\lambda > 230$ nm. Isosbestic point at 335 nm. (b) Photolysis of *trans*-(AupNBT)₂dppee (**2**) in CH₂Cl₂: *t* = 0–13 min; 420 nm filter. Isosbestic point at 335 nm.

7.600 ($J = 9.0$ Hz) and 7.496 ($J = 9.0$ Hz), that correspond to the hydrogens on the *p*-nitrobenzenethiol and indicate the formation of other thiol compounds. Based on integration, the ratio of formation of the disulfide to all other products is approximately 1:1.5. There are also two singlets, one at 4.1 ppm and another at 3.8 ppm, that represent radical recombination of the thiol and solvent radical fragments. Based on comparison with an authentic sample, the peak at 3.8 ppm is identified as C₂H₄Cl₂, from the radical combination of two CH₂Cl fragments. The peak at 4.1 ppm likely represents the hydrogens of the CH₂Cl fragment from a NO₂C₆H₄SCH₂Cl radical product formed by combination of the thiol radical and radicals from the solvent. The thiol fraction mixture was difficult to separate further. Some of these peaks may also represent breakdown products of the 4,4'-dinitrophenyldisulfide as it undergoes a photochemical reaction of its own.

Fig. 6 shows individual UV–Vis spectra that are overlaid to support the assignment of the UV–Vis peaks. The initial spectrum of the *trans*-(AupNBT)₂dppee (a solid line) shows a maximum absorbance at 385 nm which decreases as the experiment progresses. Trace b (dotted line) indicates the product of the

photolysis before separation containing *trans*-(AuCl)₂dppee and 4,4'-dinitrophenyldisulfide. The *trans*-(AuCl)₂dppee (c dash-dot line) has no absorbance at 320 nm. Trace d (dashed line) illustrates the spectrum of an authentic sample of 4,4'-dinitrophenyldisulfide for comparison. The isosbestic point implies that one species is being directly transformed into another with no intermediate. We suggest that the isosbestic point here indicates the substitution of a thiol by a chlorine radical and the formation of the 4,4'-dinitrophenyldisulfide and other thiol species that absorb at 320 nm. The *trans*-(AupNBT)₂dppee is a dinuclear molecule and it is unlikely that both *p*-nitrobenzenethiol ligands would be replaced simultaneously. We considered the possibility of an intermediate such as *trans*-(AuCl)(AupNBT)dppee whose UV–Vis spectrum is similar to the spectrum of *trans*-(AupNBT)₂dppee differing only in the intensity of the 385 nm peak because of only one *p*-nitrobenzenethiol ligand. The existence of transient peaks in the ³¹P {¹H} NMR during the photolysis reaction make this speculation reasonable. Further work is being done to identify intermediates and propose a more complete mechanism for this photochemical reaction.

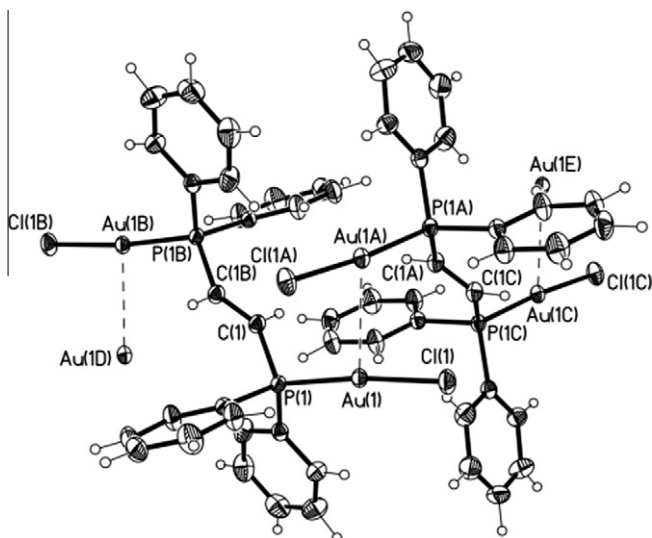


Fig. 5. Molecular structure of the photoproduct, (*trans*-(AuCl)₂dppee) (**3**) isolated from the photolysis of *trans*-(AupNBT)₂dppee ($\lambda > 230$ nm). See Table 2 for selected distances (Å) and angles (°).

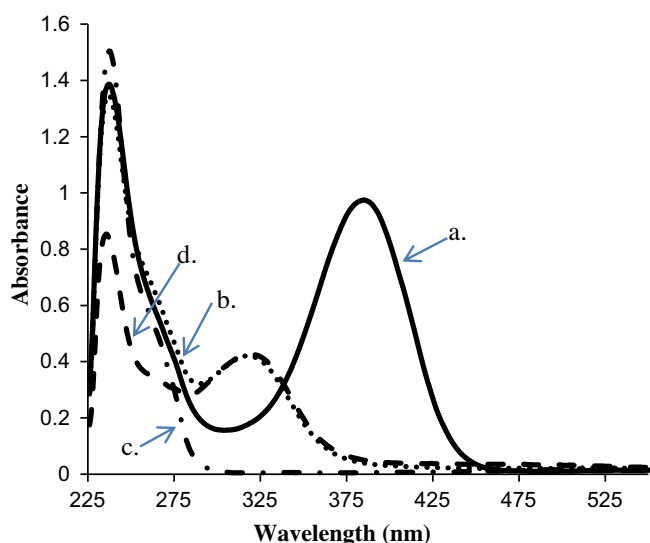


Fig. 6. Overlay of initial compound and products of photolysis reaction of *trans*-(AupNBT)₂dppee in CH₂Cl₂ (a) initial *trans*-(AupNBT)₂dppee (solid line), $c = 2.95 \times 10^{-5}$ M (b) final photoproduct, *trans*-(AuCl)₂dppee plus 4,4'-dinitrophenyl disulfide (dotted line), (c) separated *trans*-(AuCl)₂dppee product (dash-dot), and (d) authentic sample of 4,4'-dinitrophenyldisulfide (dashed line) for reference.

What is unusual here is that the same products are identified for the high energy photolysis ($\lambda > 230$ nm) and the low energy process ($\lambda > 420$ nm), despite the fact that methylene chloride does not absorb at wavelengths greater than 265 nm. We conducted several experiments to identify the photoactive species and to determine if radicals were involved as described in the next section.

3.6. Supporting experiments

3.6.1. Solvent experiments

To examine the possibility of chlorine radical formation directly from the solvent, we photolyzed the methylene chloride (2.5 ml) solvent first using a quartz cuvette and then with the 420 nm cut-off filter. The *trans*-(AupNBT)₂dppee ($c = 5.4 \times 10^{-5}$ M) was added in the dark and the progress of the reaction was monitored by

UV-Visible spectroscopy. When the solvent (CH₂Cl₂) was photolyzed with UV light for 2 min and the compound added in the dark, the UV spectrum just showed the peak at 320 nm and no peak at 385 indicating that the reaction went to completion as soon as the compound was added even though the *trans*-(AupNBT)₂dppee itself was not photochemically stimulated. This result is consistent with a mechanism in which the substitution is initiated by a chlorine radical from the solvent that displaces a thiyl radical from the complex. However, when the solvent was irradiated for 10 s or 30 s at wavelengths greater than 230 nm, the dark reaction occurred but did not go to completion, indicating that radical formation was not a catalytic chain reaction or that the rate of termination of the radicals was greater than rate of interaction with the substrate (see Supplementary data, Fig. S-2).

Under the same conditions with the 420 nm cutoff filter, there was no reaction in the dark when *trans*-(AupNBT)₂dppee was added after photolysis of the solvent for 2 min. When the solution of methylene chloride and *trans*-(AupNBT)₂dppee was exposed to the light with the 420 nm cutoff filter, the 385 nm peak diminished and the 320 nm peak grew in, indicating that the complex was necessary for the reaction to take place. Control experiments (samples in CH₂Cl₂ kept in the dark for two days at room temperature) show that *trans*-(AupNBT)₂dppee does not react with any chlorinated solvent without photolysis. We concluded from these experiments that with the 420 nm cutoff filter the excited state of the complex initiated the reaction but at wavelengths less than 265 nm, the reaction was solvent initiated. However since the gold complex also absorbs at 236 nm, both pathways could be available at the shorter wavelengths.

3.6.2. Photolysis in air and under nitrogen

The *trans*-(AupNBT)₂dppee photoreaction as described in Eq. (1) and monitored by UV-Vis spectroscopy, occurs when the solution was photolyzed in air or under an inert atmosphere, nitrogen. The rates of the photochemical reaction in air or under nitrogen are similar implying that oxygen does not quench the reaction nor does it accelerate it (see Supplementary data, Fig. S-3). Often oxygen has a quenching effect on metal based photochemical reactions [38] but we do not observe this here.

3.6.3. Radical trap experiments

DPPH (α, α -diphenyl- β -picrylhydrazyl) was used to detect if radicals were formed during the reaction. When a molar excess of DPPH was added to *trans*-(AupNBT)₂dppee in methylene chloride and the sample was photolyzed in quartz, there was little change in the rate of photolysis, 2×10^{-6} mL⁻¹ s⁻¹, measured by the change in absorbance at 385 nm representing the decrease in concentration of *trans*-(AupNBT)₂dppee (see Supplementary data, Fig. S-4). If the initiating step in the photolysis is the homolytic cleavage of the C–Cl bond in the solvent and the solvent is in great excess compared to the complex, it is not surprising that there is no measurable change in the rate of the reaction. However there was a clear decrease in the DPPH absorbance at 550 nm, indicating that the DPPH was indeed trapping radicals.

When DPPH was added to a sample of *trans*-(AupNBT)₂dppee in methylene chloride that was photolyzed with the 420 nm cutoff filter, the concentration of *trans*-(AupNBT)₂dppee was reduced to 4.99e-5M (a 17.5% reduction) after 12 min whereas in the control sample (without DPPH) the concentration was 7.05e-6M, (a 87.5% reduction) clearly indicating that DPPH was slowing the photoreaction. The decrease in absorbance at 550 nm, where DPPH absorbs, was clear as well, indicating that DPPH was reacting with radicals.

The solvent experiments support our hypothesis that at high energy chlorine radicals from direct photolysis of the solvent initiate the reaction. Other researchers have observed this solvent

initiated photolysis in addition reactions to metals [39]. Examples also show that metal complexes, excited at wavelengths where solvents do not absorb, can abstract chlorine radicals from the solvent [40]. Pignolet's work [41] with photolysis of metal dithiocarbamates explains the substitution of Cl for a dithiocarbamate by a LMCT reduction of the metal and the reduced complex abstracting a Cl radical from the solvent. It is interesting to note that the dithiocarbamate disulfide was identified as a minor product of this photolysis. Van der Graaf [42] discusses the abstraction of a chlorine from the solvent by a rhenium radical formed from excitation of a bimetallic complex at wavelengths where the solvent does not absorb. Giuffrida et al. [43] show a solvent initiated process for $\text{Sr}(\text{hfac})_2\text{TG}$ ($\text{hfac} = 1,1,1,5,5,5$ -hexafluoro-2,4-pentanedionato and $\text{TG} = \text{tetraglyme} = 2,5,8,11,14$ -pentaioxapentadecane) at high energies, but a solvent-assisted reaction involving electron transfer from an excited triplet state of the complex to the solvent at lower energies: both processes giving the same product, SrCl_2 , by different mechanisms.

3.7. Summary of *trans*-(*AupNBT*)₂*dppee* photoprocess

Formation of the *trans*-(AuCl)₂*dppee* is not that interesting in itself, in fact; it is the starting material for all our syntheses and it is easily prepared by reduction of HAuCl_4 and addition of *trans*-bis(diphenylphosphino)ethylene. The interesting point is that we are producing the same product by two different pathways dependent on the wavelength of excitation. A Au–S bond is stronger than a Au–Cl bond [44], and the *p*-nitrobenzenethiol is a much “softer” ligand and is expected to have a better orbital overlap with the gold than the “harder” chloride ligand. Thermodynamically, we are driving the reaction “uphill” by absorption of energy, even with visible wavelengths. If we look at a rough bond breaking/bond making scenario, considering that cleavage of one C–Cl bond in the solvent will initiate other radicals, we look at putting energy into break one C–Cl bond (307.8 kJ m^{-1}) plus two Au–S bonds (836 kJ m^{-1}) and getting energy from formation of two Au–Cl bonds (686 kJ m^{-1}) and one disulfide bond (230 kJ m^{-1}) giving an overall ΔH of $+227.8 \text{ kJ m}^{-1}$ which is compensated even by energies of $\lambda > 420 \text{ nm}$ ($E = 285 \text{ kJ m}^{-1}$).

3.8. Computational results

DFT and TDDFT calculations performed on the model of complexes, *cis* and *trans*-(*AupNBT*)₂*dppee* $\text{C}_{14}\text{H}_{14}\text{Au}_2\text{N}_2\text{O}_4\text{P}_2\text{S}_2$, in GAUSSIAN 09 were used to explain the observed photochemical reactions and the emission spectra of the complexes. The lowest energy geometry of the *cis* isomer model complex used coordinates given by the crystal structure for *cis*-(*AupNBT*)₂*dppee*, including the 3.00 Å gold–gold distance. The HOMO and the HOMO – 1 of *cis*-(*AupNBT*)₂*dppee* are clearly on the thiol ligand, mostly S p_z with some electron density on the gold atoms (see Fig. 7). The LUMO is primarily ethylene π^* with some bonding and antibonding interactions on the gold atoms. The lowest energy singlet excitation for *cis*-(*AupNBT*)₂*dppee* is at 542.71 nm and is a HOMO to LUMO transition. There are several low energy triplet states (at 556.56, 540.76 nm) that are also HOMO (or HOMO – 1) to LUMO that could initiate the isomerization. Because of heavy metal spin orbit coupling, it is likely that a triplet state is involved in the photoprocess, so population of higher energy states available with the excitation in quartz could readily undergo intersystem crossing to a lower energy triplet with ethylene π^* character. Higher excited states, the LUMO + 1 or LUMO + 2 do not have any ethylene π^* character so it is unlikely that these states would initiate the isomerization. These data suggest that the lowest energy transition in the *cis*-(*AupNBT*)₂*dppee* is a ligand to ligand transition (LLCT) affected by a ligand to metal–metal (LMMCT) transition because of the electron density between the

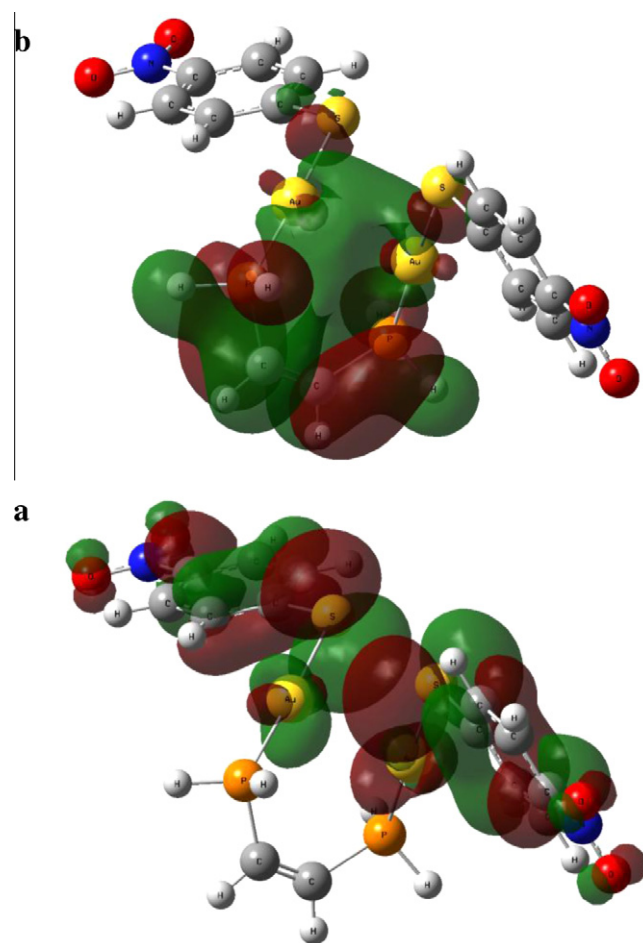


Fig. 7. Frontier orbitals, HOMO(a) and LUMO(b), of the model complex ($\text{C}_{14}\text{H}_{14}\text{Au}_2\text{N}_2\text{O}_4\text{P}_2\text{S}_2$) of *cis*-(*AupNBT*)₂*dppee* based on the TDDFT calculation using LANL2DZ basis set, 6-311(d,p) basis set for non metal atoms, and the B3LYP correlation function.

gold atoms and the obvious necessity of weakening the gold–gold attraction for the isomerization.

It is interesting to note that results of a different DFT calculation on the model *cis*-(*AupNBT*)₂*dppee* structure that did not confine the gold–gold distance to 3.0 Å had a slightly higher energy and a gold–gold distance of 3.379 Å, close enough for weak gold–gold interactions. Both calculations indicated a similar orbital composition but the initial excited states (1–5) of the 3.379 Å structure are markedly blue shifted relative to the structure with gold–gold distance of 3.0 Å (see Supplementary data; S-7). Gold–gold interactions are weak, about the same energy as hydrogen bonds, and although the distance may vary in solution compared to the crystal, the closer gold–gold distance not only facilitates the isomerization but appears to allow absorption and emission at lower energies.

DFT and TDDFT calculations were done on the model complex of *trans*-(*AupNBT*)₂*dppee* using the IEP-PCM for the solvent methylene chloride to investigate the basis for our experimental results (see Supplementary data; S-8). The HOMO and the HOMO – 1 are close in energy alternating electron density on the two *p*-nitrobenzenethiol ligands of the dinuclear complex, primarily on the sulfur p_z but with some minor electron density on the gold atoms (see Fig. 8). The LUMO and the LUMO + 1 of the complex are $p_z\pi^*$ on the NO_2 and around the phenyl ring of the *p*-nitrobenzenethiol. This suggests that the lowest energy excited state is an intraligand transition where the sulfur donates electron density to the NO_2 of

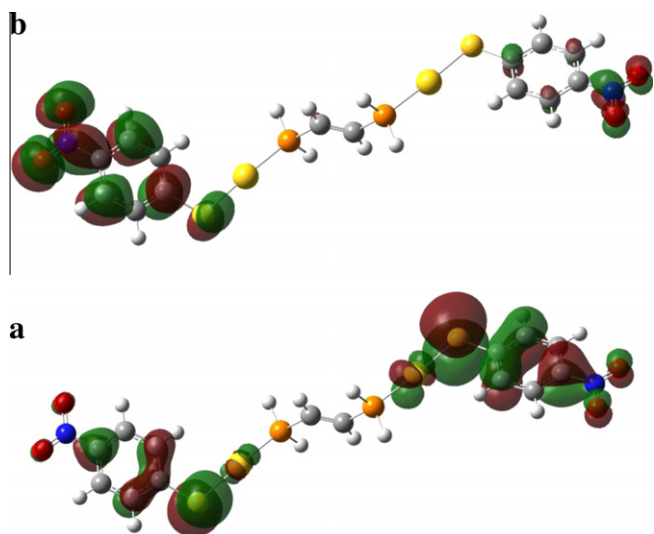


Fig. 8. Frontier orbitals, HOMO(a) and LUMO(b), of the model complex ($C_{14}H_{14}Au_2N_2O_4P_2S_2$) of *trans*-(AupNBT)₂dppee based on the TDDFT calculation using LANL2DZ basis set, 6-311(d,p) basis set for non metal atoms, and the B3LYP correlation function.

the same ligand. The three lowest energy triplet transitions in the *trans*-(AupNBT)₂dppee are all HOMO to LUMO (or H – 1 to L + 1) which are also *p*-nitrobenzenethiol centered transitions. Population of the LUMO would take electron density from the sulfur, weakening the gold–sulfur bond, allowing substitution at the gold, which is what we see experimentally. The transition with the highest oscillator strength (0.8069) is a singlet transition at 390.41 nm and the excitation with the highest coefficient is HOMO to LUMO (see Supplementary data; S-8). The reaction happens also at wavelengths greater than 420 nm and there are two triplet states at 496.99 and 496.50 nm that are also HOMO to LUMO, and could initiate the same substitution reaction. As in the *cis* isomer, spin–orbit coupling makes occupation of triplet states likely. The calculations support the assertion that the excited state involves an intraligand charge transfer (LLCT) from the $p_z\pi$ of the sulfur to the $p_z\pi^*$ of the NO₂. In the excited states, there is no electron density on the gold until the LUMO + 2 or above, making the possibility of an LMCT less probable.

Computations were done on the mixed ligand complex, *trans*-(AuCl)(AupNBT)dppee in methylene chloride to explore the existence of this species as a possible intermediate. The first singlet transition is HOMO to LUMO and both orbitals are very similar to the frontier orbitals of the *trans*-(AupNBT)₂dppee as expected because of the dominance of the *p*-nitrobenzenethiol ligand. There is a singlet transition at 387.41 nm, with an oscillator strength of 0.4758 that is HOMO to LUMO. Again there are several triplet states that populate the LUMO at lower energies that would explain the photolysis with the 420 nm filter.

3.8.1. Absorbance

The theoretical absorption spectra derived from the TDDFT calculation of both the *cis* and *trans*-(AupNBT)₂dppee reflect what we see experimentally (see Supplementary data; S-5). The absorbance spectrum of *cis*-(AupNBT)₂dppee shows the most favored transition with an oscillator strength of 0.4260 is a singlet at 393.70 nm compared to our experimental absorbance maximum at 400 nm. The theoretical molar absorptivity of 3.0×10^4 is close to our experimental value of 3.25×10^4 M cm⁻¹. For *trans*-(AupNBT)₂dppee the transition with the highest oscillator strength occurs at 390.41 nm, close to our experimental maximum at 385 nm. The molar absorptivity is slightly higher at 3.6×10^4

than our experimental value of 3.3×10^4 M cm⁻¹. This agreement suggests that the calculation is an adequate model for our system.

3.9. Photophysical properties of the *cis* and *trans*-(AupNBT)₂dppee isomers

Although there are similarities between the two isomers (see Table 3 for specific data), such as absorbance in the visible and the red shift in the emission going from solution to solid state, the geometry and the nature of the excited states are clearly different. Many of the similar features can be attributed to the *p*-nitrobenzenethiol ligand that dominates the HOMO of both of these complexes. The differences in reactivity are likely a result of the *cis* geometry facilitating the gold–gold interaction, making the LUMO ethylene π^* . In contrast, in the *trans* isomer intramolecular interactions are not possible and the donor/acceptor relationship of the *p*-nitrobenzenethiol lowers the energy of the LUMO enough so the ethylene π^* orbital is higher energy. Studies are underway to evaluate the reactivity of other thiol ligands with this system to determine if the *p*-nitrobenzenethiol is unique in its photochemical reactivity.

3.9.1. Emission

When excited at 385 nm, *trans*-(AupNBT)₂dppee emits at 505 nm at room temperature in methylene chloride and at 600 nm in the solid state (with KBr) (see Fig. 9). Based on the TDDFT calculation, the emission in solution for *trans*-(AupNBT)₂dppee is likely from a triplet state that absorbs at 496.99 nm and is a LUMO or the LUMO + 1 to the HOMO or HOMO – 1, all *p*-nitrobenzenethiol transitions. Unlike other assignments for gold(I) thiol complexes where the lowest energy transition is characterized as an LMCT, this emission is dominated by a LLCT, an assignment that has been observed before with this ligand [32b].

Table 3

Photochemical and photophysical data for *cis*-(AupNBT)₂dppee (1) and *trans*-(AupNBT)₂dppee (2).

| | Absorbance λ_{abs} (nm) (ϵ , M ¹ cm ⁻¹) | Emission λ_{em} (nm) |
|---|--|---|
| 1 | 400 nm (32 500) 236 nm (43 700) | 510 nm (in CH ₂ Cl ₂) 588 nm (solid state in KBr) |
| 2 | 385 nm (32 900) 236 nm (51 500) | 505 nm (in CH ₂ Cl ₂) 600 nm (solid state in KBr) |

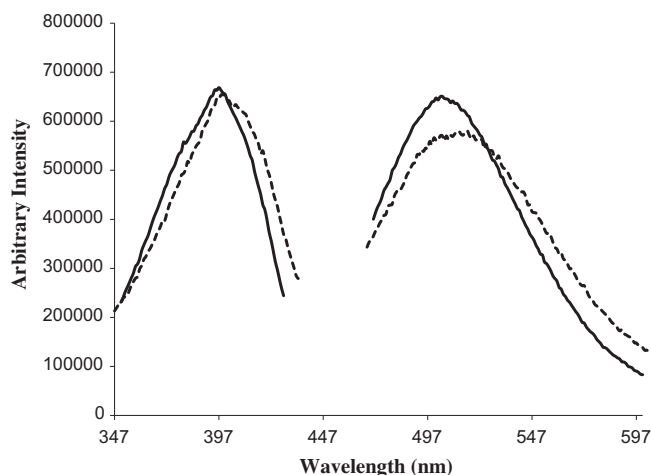


Fig. 9. Emission and excitation spectra of *cis*-(AupNBT)₂dppee (dashed line: emission at 510 nm), and *trans*-(AupNBT)₂dppee (solid line: emission at 505 nm).

As another way of characterizing the excited state, we followed the photolysis reaction by UV–Vis and emission spectroscopy as the reaction was progressing. When *trans*-(AuNBT)₂dppee was photolyzed in quartz, the emission intensity of the 505 nm peak initially increased, reaching a maximum at *t* = 45 s, then decreased rapidly to a minimum at *t* = 60 s while a peak grew in at 437 nm (see Supplementary data, Fig. S-6). By *t* = 60 s the 385 peak in the UV–Vis had decreased to virtually zero and the peak at 320 had grown in, indicating that the reaction was complete. The initial increase in emission intensity is interesting, suggesting a different emitting species from the initial *trans*-(AuNBT)₂dppee, perhaps an intermediate not apparent in the UV–Vis spectrum. This species then changes quickly, forming the characterized products. This experiment supports the hypothesis that the state responsible for the low energy emission is the same state that initiates the photochemical ligand substitution.

The complex, *cis*-(AuNBT)₂dppee, has a 510 nm emission in methylene chloride at room temperature when excited at 400 or 420 nm and a 588 nm emission in the solid state. The lowest energy emission from the TDDFT calculation of *cis*-(AuNBT)₂dppee with the 3.0 Å gold–gold distance was at 556.56 nm, in between the solution and the solid state values. The discrepancy between experimental and theoretical emission could be explained by this structure being more similar to the solid state crystal with the gold–gold distance of 3.00 Å rather than a more flexible gold–gold distance that might exist in solution. The TDDFT results of the more relaxed *cis* structure (gold–gold distance = 3.379 Å), has the lowest triplet emission at 536.11 nm, closer to the experimental value.

4. Conclusion

We have synthesized and characterized a pair of *cis* and *trans* dinuclear gold isomers and investigated their photochemical and photophysical properties. The complex, *cis*-(AuNBT)₂dppee, has an intramolecular gold–gold distance of 3.0036(3) Å and isomerizes to the *trans* isomer with light of wavelengths greater than 230 nm as well as $\lambda > 420$ nm. The complex, *trans*-(AuNBT)₂dppee, crystallizes as a dimer with an intermolecular gold–gold distance of 3.1201(4) Å and undergoes a wavelength dependent photochemical reaction in chlorinated solvents. This reaction produces the same products, *trans*-(AuCl)₂dppee, 4,4'-dinitrophenyldisulfide, and thiol radical products, at $\lambda > 230$ nm and at $\lambda > 420$ nm, but through different radical mechanisms. The crystal of the *trans*-(AuCl)₂dppee photoproduct is an infinite chain polymer with intermolecular gold–gold distances of 3.0203(2) Å. DFT and TDDFT calculations support the assignment of a LLCT (Sp_z → ethylene π*) modified by a LMMCT (Sp_z → Au–Au) transition for the *cis*-(AuNBT)₂dppee and an LLCT (Sp_z → NO₂ p_zπ*) for the *trans*-(AuNBT)₂dppee. The photochemical stability of gold–thiol bonds has implications for the use of gold–thiol drugs as well as the many surface applications that rely on gold–thiol attachments.

Acknowledgements

JBF thanks Vermont EPSCoR for partial funding of this project. JBF is grateful to Dr. Alice E. Bruce for helpful discussions. EVD is grateful to the National Science Foundation (CHE-1152441) for financial support.

Appendix A. Supplementary material

Supplementary data associated with this article can be found, in the online version, at <http://dx.doi.org/10.1016/j.ica.2012.03.030>.

References

- [1] C.F. Shaw, Chem. Rev. 99 (1999) 2589.
- [2] (a) F. Caruso, C. Pettinari, F. Paduano, R. Villa, F. Marchetti, E. Monti, M. Rossi, J. Med. Chem. 51 (2008) 1584; (b) I. Ott, X. Qian, Y. Xu, D.H.W. Vlecken, I.J. Marques, D. Kubutat, J. Will, W.S. Sheldrick, P. Jesse, A. Prokop, C.P. Bagowski, J. Med. Chem. 52 (2009) 763.
- [3] (a) V. Gandin, A.P. Fernandes, M.P. Rigobello, B. Dani, F. Sorrentino, F. Tisato, M. Björnstedt, A. Bindoli, A. Sturaro, R. Rella, Biochem. Pharmacol. 79 (2010) 90; (b) K.P. Bhabak, G. Mugesh, Inorg. Chem. 48 (2009) 2449.
- [4] (a) D.A. Harvey, W.F. Kean, C.J. Lock, D. Signal, Lancet (1983) 470; (b) M.C. Grootveld, P.J. Sadler, J. Inorg. Biochem. 19 (1983) 51.
- [5] (a) B.J. Henz, T. Hawa, M.R. Zachariah, Langmuir 24 (2008) 773; (b) W.R. Browne, T. Kudernac, N. Katsonis, J. Areephong, J. Hjelm, B.L. Feringa, J. Phys. Chem. 112 (2008) 1183.
- [6] (a) M.J. Katz, T. Ramnial, H. Yu, D.B. Leznoff, J. Am. Chem. Soc. 130 (2008) 10662; (b) J. Schneider, Y. Lee, J. Perez, W.W. Brennessel, C. Flaschenriem, R. Eisenberg, Inorg. Chem. 47 (2008) 957.
- [7] (a) C. Chen, Y. Lin, C. Wang, H. Tzeng, C. Wu, Y. Chen, C. Chen, L. Chen, Y. Wu, J. Am. Chem. Soc. 128 (2006) 3709; (b) J.D.E.T. Wilton-Ely, Dalton Trans. (2008) 25.
- [8] (a) S. Sanz, L.A. Jones, F. Mohr, M. Laguna, Organometallics 26 (2007) 952; (b) N. Meyer, E. Schuh, F. Mohr, Annu. Rep. Prog. Chem. 106 (2010) 255.
- [9] (a) S. Cha, J. Kim, K. Kim, J. Lee, Chem. Mater. 19 (2007) 6297; (b) W.J. Hunks, M.C. Jennings, R.J. Puddephatt, Inorg. Chem. 41 (2002) 4590; (c) B. Tzeng, H. Yeh, Y. Wu, J. Kuo, G. Lee, S. Peng, Inorg. Chem. 45 (2006) 591.
- [10] (a) V.W.-W. Yam, C.-L. Chan, C.-K. Li, M.-C. Wong, Coord. Chem. Rev. 216–217 (2001) 173; (b) C.-M. Che, S.-W. Lai, Luminescence and photophysics of gold complexes, in: F. Mohr (Ed.), Gold Chemistry. Applications and Future Directions in the Life Sciences, Wiley-VCH, Weinheim, 2009.
- [11] J.B. Foley, A.E. Bruce, M.R.M. Bruce, J. Am. Chem. Soc. 117 (1995) 9596.
- [12] J.B. Foley, S.E. Gay, M.J. Vela, B.M. Foxman, A.E. Bruce, M.R.M. Bruce, Eur. J. Inorg. Chem. 31 (2007) 4946.
- [13] P. Schwerdtfeger, A.E. Bruce, M.R.M. Bruce, J. Am. Chem. Soc. 120 (1998) 6587.
- [14] P. Pykkö, J. Li, N. Runeberg, Chem. Phys. Lett. 218 (1,2) (1994) 133.
- [15] (a) P.E. Hoggard, Coord. Chem. Rev. 159 (1997) 235; (b) A. Vogler, H. Kunkely, Coord. Chem. Rev. 230 (2002) 243.
- [16] N. Meyer, C.W. Lehmann, T.K.-M. Lee, J. Rust, V.W.-W. Yam, F. Mohr, Organometallics 28 (10) (2009) 2931; (b) F. Mohr, S.H. Privér, S.K. Bhargava, M.A. Bennett, Coord. Chem. Rev. 250 (2006) 1851.
- [17] (a) R. Usón, A. Laguna, M. Laguna, J. Jiménez, P.G. Jones, J. Chem. Soc., Dalton Trans. (1991) 1361; (b) H.H. Murray, J.P. Fackler Jr, Inorg. Chim. Acta 115 (1986) 207; (c) H. Schmidbauer, P. Jandik, Inorg. Chim. Acta 74 (1983) 97.
- [18] (a) R.G. Raptis, H.H. Murray, R.J. Staples, L.C. Porter, J.P. Fackler Jr., Inorg. Chem. 32 (1993) 5576; (b) J.D. Basil, H.H. Murray, J.P. Fackler Jr, J. Tocher, A.M. Mazany, B. Trzcinska-Bancroft, H. Knachel, D. Budis, T.J. Delord, D.O. Marler, J. Am. Chem. Soc. 107 (1985) 6908.
- [19] (a) R.H. Hill, R.J. Puddephatt, J. Am. Chem. Soc. 107 (1985) 1218; (b) S. Sathiyabalan, P.E. Hoggard, Inorg. Chem. 34 (1995) 4562; (c) T.H. Nguyen, P.J. Shannon, P.E. Hoggard, Inorg. Chim. Acta 291 (1999) 136.
- [20] (a) E.M. Jaryszak, P.E. Hoggard, Inorg. Chim. Acta 282 (1998) 217; (b) P.E. Hoggard, A.J. Bridgeman, H. Kunkely, A. Vogler, Inorg. Chim. Acta 357 (2004) 639.
- [21] (a) C.C. Tong, M. Winkelman, A. Jain, S.P. Jensen, P.E. Hoggard, Inorg. Chim. Acta 226 (1994) 247; (b) N.E. Leadbeater, C. Jones, Transition Met. Chem. 25 (2000) 99; (c) G.L. Miessler, L.H. Pignolet, Inorg. Chem. 18 (1979) 210.
- [22] (a) C.R. Bock, M.S. Wrighton, Inorg. Chem. 16 (1977) 1309; (b) P.E. Hoggard, M. Gruber, A. Vogler, Inorg. Chim. Acta 346 (2003) 137.
- [23] J.M. Stegge, S.M. Woessner, P.E. Hoggard, Inorg. Chim. Acta 250 (1996) 385.
- [24] K.W. Lee, P.E. Hoggard, Inorg. Chem. 32 (1993) 1877.
- [25] (a) R. Narayanaswamy, M.A. Young, E. Parkhurst, M. Ouellette, M.E. Kerr, D.M. Ho, R.C. Elder, A.E. Bruce, M.R.M. Bruce, Inorg. Chem. 32 (1993) 2202; (b) W.B. Jones, J. Yuan, R. Narayanaswamy, M.A. Young, R.C. Elder, A.E. Bruce, M.R.M. Bruce, Inorg. Chem. 34 (1995) 1996; (c) J.M. Forward, D. Bohmann, J.P. Fackler Jr., R.J. Staples, Inorg. Chem. 34 (1995) 6330.
- [26] (a) P. Pykkö, Chem. Rev. 97 (1997) 597; (b) H. Schmidbauer, Chem. Soc. Rev. (1995) 391; (c) D.J. Gorin, F.D. Toste, Nature 446 (2007) 395.
- [27] C.-K. Li, X.-X. Lu, K.M.-C. Wong, P.G. Chan, N. Zhu, W.-W. Yam, Inorg. Chem. 43 (2004) 7421.
- [28] P.G. Jones, Acta Cryst. B36 (1980) 2775.
- [29] D.S. Eggleston, J.V. McArdle, G.E. Zuber, J. Chem. Soc., Dalton Trans. (1987) 677.
- [30] M.J. Frisch, G.W. Trucks, H.B. Schlegel, G.E. Scuseria, M.A. Robb, J.R. Cheeseman, G. Scalmani, V. Barone, B. Mennucci, G.A. Petersson, H. Nakatsuji, M. Caricato, X. Li, H.P. Hratchian, A.F. Izmaylov, J. Bloino, G. Zheng, J.L. Sonnenberg, M. Hada, M. Ehara, K. Toyota, R. Fukuda, J. Hasegawa, M. Ishida, T. Nakajima, Y. Honda, O. Kitao, H. Nakai, T. Vreven, J.A. Montgomery Jr., J.E. Peralta, F. Ogliaro, M. Bearpark, J.J. Heyd, E. Brothers, K.N. Kudin, V.N. Staroverov, R. Kobayashi, J.

- Normand, K. Raghavachari, A. Rendell, J.C. Burant, S.S. Iyengar, J. Tomasi, M. Cossi, N. Rega, J.M. Millam, M. Klene, J.E. Knox, J.B. Cross, V. Bakken, C. Adamo, J. Jaramillo, R. Gomperts, R.E. Stratmann, O. Yazyev, A.J. Austin, R. Cammi, C. Pomelli, J.W. Ochterski, R.L. Martin, K. Morokuma, V.G. Zakrzewski, G.A. Voth, P. Salvador, J.J. Dannenberg, S. Dapprich, A.D. Daniels, O. Farkas, J.B. Foresman, J.V. Ortiz, J. Cioslowski, D.J. Fox, GAUSSIAN 09, Revision A.02, Gaussian, Inc., Wallingford CT, 2009.
- [31] C. King, J.-C. Wang, M.N.I. Khan, J.P. Fackler Jr., *Inorg. Chem.* 28 (1989) 2145.
- [32] (a) S.M. Bessey, M. Aghamoosa, G.S.P. Garusinghe, A. Chandrasoma, A.E. Bruce, M.R.M. Bruce *Inorg. Chim. Acta* 363 (2010) 279;
(b) C.-H. Li, S.F. Kui, I.H.T. Sham, S.S.-Y. Chui, C.-M. Che, *Eur. J. Inorg. Chem.* (2008) 2421.
- [33] R.S. Sengar, V.N. Nemykin, P. Basu, *New J. Chem.* 27 (2003) 1115.
- [34] (a) H. Schmidbauer, A. Schier, *Chem. Soc. Rev.* 37 (2008) 1931;
(b) P. Pyykkö, *Chem. Rev.* 88 (1988) 563.
- [35] S. Onaka, Y. Katsukawa, M. Yamashita, *Chem. Lett.* (1998) 525.
- [36] S. Onaka, Y. Katsukawa, M. Shiotsuka, O. Kanegawa, M. Yamashita, *Inorg. Chim. Acta* 312 (2001) 100.
- [37] (a) E.M. Gussenhoven, J.C. Fettingner, D.M. Pham, M.M. Malwitz, A.L. Balch, *J. Am. Chem. Soc.* 127 (2005) 10838;
(b) R.L. White-Morris, M.M. Olmstead, S. Attar, A.L. Balch, *Inorg. Chem.* 44 (2005) 5021;
- (c) D.R. Smyth, B.R. Vincent, E.R.T. Tienkink, *Cryst. Growth Des.* 1 (2) (2001) 113.
- [38] D. Sandrini, M. Maestri, V. Balzani, L. Chassot, A. Von Zelewsky, *J. Am. Chem. Soc.* 109 (1987) 7720.
- [39] (a) S. Whang, T. Estrada, P.E. Hoggard, *Photochem. Photobiol.* 79 (2004) 356;
(b) A.L. Le, Patrick E. Hoggard, *Photochem. Photobiol.* 84 (2008) 86.
- [40] (a) R.M. Laine, P.C. Ford, *Inorg. Chem.* 16 (1977) 388;
(b) Y.A. Mikheev, V.P. Pustoshnyi, D.Y. Toptygin, *Russ. Chem. Bull.* 25 (1976) 1962;
(c) C. Aprile, M. Boronat, B. Ferrer, A. Corma, H. Garcia, *J. Am. Chem. Soc.* 128 (2006) 8388.
- [41] (a) G.L. Miessler, E. Zuebis, L.H. Pignolet, *Inorg. Chem.* 17 (1978) 3636;
(b) G.L. Miessler, G. Stuk, K.W. Given, M.C. Palazzotto, L.H. Pignolet, *Inorg. Chem.* 15 (1976) 1982.
- [42] T. van der Graaf, A. van Rooy, D.J. Stufkens, A. Oskam, *Inorg. Chim. Acta* 187 (1991) 133.
- [43] S. Guiffrida, L.L. Costanzo, G.G. Condorelli, G. Ventimiglia, I.L. Fragalà, *Inorg. Chim. Acta* 358 (2005) 1873.
- [44] Bond energies are from Lange's Handbook of Chemistry, 15th ed., John Dean, p 4.45. Bond energies are for gas state dinuclear molecules and are meant as an approximation.
- [45] P.A. Bates, J.M. Waters, *Inorg. Chim. Acta* 98 (1985) 125.